Photon Statistics of Propagating Thermal Microwaves

J. Goetz,[1,2,*] S. Pogorzalek,[1,2] F. Deppe,[1,2,3] K. G. Fedorov,[1,2] P. Eder,[1,2,3] M. Fischer,[1,2,3] F. Wulschner,[1,2] E. Xie,[1,2,3] A. Marx,[1] and R. Gross[1,2,3,†]

[1]*Walther-Meißner-Institut, Bayerische Akademie der Wissenschaften, 85748 Garching, Germany*

[2]*Physik-Department, Technische Universität München, 85748 Garching, Germany*

[3]*Nanosystems Initiative Munich (NIM), Schellingstraße 4, 80799 München, Germany*

(Received 29 September 2016; revised manuscript received 30 December 2016; published 8 March 2017)

In experiments with superconducting quantum circuits, characterizing the photon statistics of propagating microwave fields is a fundamental task. We quantify the $n^2 + n$ photon number variance of thermal microwave photons emitted from a blackbody radiator for mean photon numbers, $0.05 \lesssim n \lesssim 1.5$. We probe the fields using either correlation measurements or a transmon qubit coupled to a microwave resonator. Our experiments provide a precise quantitative characterization of weak microwave states and information on the noise emitted by a Josephson parametric amplifier.

DOI: 10.1103/PhysRevLett.118.103602

As propagating electromagnetic fields in general [1–3], propagating microwaves with photon numbers on the order of unity are essential for quantum computation [4,5], communication [6], and illumination [7–10] protocols. Because of their omnipresence in experimental setups, the characterization of thermal states is especially relevant for many applications [11–14]. Specifically in the microwave regime, sophisticated experimental techniques for their generation at cryogenic temperatures, their manipulation, and their detection have been developed in recent years. In this context, an important aspect is the generation of propagating thermal microwaves using thermal emitters [15–17]. These emitters can be spatially separated from the setup components used for manipulation and detection [18,19], which allows one to individually control the emitter and the setup temperature. Because of the low energy of microwave photons, the detection of these fields typically requires the use of near-quantum-limited amplifiers [20–23], cross-correlation detectors [17,18,24], or superconducting qubits [25–28].

The unique nature of propagating fields is reflected in their photon statistics, which is described by a probability distribution either in terms of the number states or in terms of its moments. The former were studied by coupling the field to an atom or qubit and measuring the coherent dynamics [29–31] or by spectroscopic analysis [32]. The moment-based approach requires knowledge on the average photon number n and its variance, $\mathrm{Var}(n) = \langle n^2 \rangle - \langle n \rangle^2$, to distinguish many states of interest. To this end, the second-order correlation function $g^{(2)}(\tau)$ has been measured to analyze the photon statistics of thermal [33–35] or quantum [36–38] emitters ever since the groundbreaking experiments of Hanbury Brown and Twiss [39,40]. While these experiments use the time delay τ as the control parameter, at microwave frequencies, the photon number n can be controlled conveniently [15,32,41–44]. In the specific case of a thermal field at frequency ω, the Bose-Einstein distribution yields $n(T) = [\exp(\hbar\omega/k_B T) - 1]^{-1}$ and $\mathrm{Var}(n) = n^2 + n$, which can be controlled by the temperature T of the emitter. In practice, one wants to distinguish this relation from both the classical limit, $\mathrm{Var}(n) = n^2$, and the Poissonian behavior, $\mathrm{Var}(n) = n$, characteristic for coherent states [41] or shot noise [45,46]. Hence, as shown in Fig. 1, the most relevant regime for experiments is $n \lesssim 1$, which translates into temperatures between 100 mK and 1 K at approximately 6 GHz for the thermal emitter [28].

In this Letter, we experimentally confirm the theoretically expected photon number variance $\mathrm{Var}(n)$ of thermal microwave fields for $n \lesssim 1.5$ using two fundamentally distinct experimental setups. To this end, we first use a superconducting transmon qubit [47] interacting with the propagating fields via a dispersively coupled microwave resonator. Differently from approaches relying on the coherent dynamics [29–31], where decoherence is detrimental, the additional qubit dephasing rate, induced by the field, directly reflects the photon number variance in our experiments. We furthermore get access to finite-time correlations for fields with Poissonian photon statistics because the resonator mediates different decay constants for the photon-photon correlator of incoherent and coherent

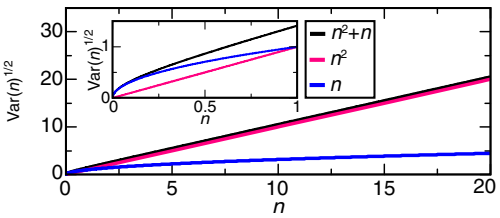

FIG. 1. Photon number correlations. $[\mathrm{Var}(n)]^{1/2}$ plotted versus the photon number for thermal fields (black), their classical limit (red), and coherent states (blue). The inset shows the regime that we capture in our experiments.

noises. In particular, we find the expected factor of two between the dephasing rates caused by coherent states and shot noise. With the second setup, we extract the super-Poissonian photon statistics of propagating thermal microwaves from direct correlation measurements and from measurements using a near-quantum-limited Josephson parametric amplifier (JPA) [21,48] as a preamplifier. The results show that the noise added by the JPA inevitably alters the photon statistics of the amplified field. Our results provide a quantitative picture of propagating thermal microwaves, which is especially relevant for the characterization of more advanced quantum states in the presence of unavoidable thermal background fields. With respect to superconducting qubits, we gain systematic insight into a dephasing mechanism which may become relevant for state-of-the-art devices with long coherence times [49,50].

In our experiments, we generate the thermal fields using a temperature-controllable, 50 Ω-matched attenuator acting as a blackbody emitter. This emitter is thermally only weakly coupled to the 35 mK base temperature stage of a dilution refrigerator. Heating the attenuator up to 1.5 K results in the emission of thermal microwave radiation with a photon number stability, $[\mathrm{Var}(n)]^{1/2}/n \lesssim 0.01$. In addition, we investigate coherent states emitted from a microwave source and white electronic shot noise with a 200 MHz bandwidth, generated by an arbitrary function generator (AFG). The AFG output is upconverted to a center frequency of 6.05 GHz (see Ref. [51] for details). For coherent states and shot noise, the photon number entering the cryostat is proportional to the power set at the microwave source or the AFG, respectively.

To measure the photon number fluctuations of propagating microwaves, we enhance their lifetime by trapping them inside a coplanar waveguide resonator. The latter is dispersively coupled to a superconducting transmon qubit acting as a sensitive detector [see Fig. 2(a)]. The transmon qubit is frequency tunable and operated at its maximum transition frequency $\omega_q/2\pi = 6.92$ GHz. The resonator with resonance frequency, $\omega_r/2\pi = 6.07$ GHz, is characterized by its external coupling and internal loss rate, $\kappa_x/2\pi = 8.5$ MHz and $\kappa_i/2\pi \simeq 50$ kHz. The dispersive interaction Hamiltonian reads $\mathcal{H}_{\mathrm{int}} = \hbar\chi[n_r + 1/2]\hat{\sigma}_z$, where [47] $\chi \equiv [g^2/\delta][\alpha/(\delta+\alpha)] \simeq -2\pi \times 3.11$ MHz. In this expression, $g/2\pi \simeq 67$ MHz is the qubit-resonator coupling, $\alpha/2\pi \simeq -315$ MHz is the transmon anharmonicity, and $\delta \equiv \omega_q - \omega_r$ is the detuning. Following input-output formalism [63,64], the photon number fluctuations $n(\tau)$ of the incident fields have the same statistics as $n_r(\tau)$ for our sample parameters. Because these fluctuations couple to the qubit via the Pauli operator $\hat{\sigma}_z$, they introduce qubit dephasing characterized by the photon-photon correlator, $\mathcal{C}(\tau) \equiv \langle n_r(0)n_r(\tau)\rangle - \langle n_r(0)\rangle^2$ [65]. For all microwave states discussed here, $\mathcal{C}(\tau) = \mathrm{Var}(n_r)\exp(-\tilde{\kappa}\tau)$ factorizes into the photon number variance and a temporal decay with rate $\tilde{\kappa}$ due to the resonator [51]. For incoherent

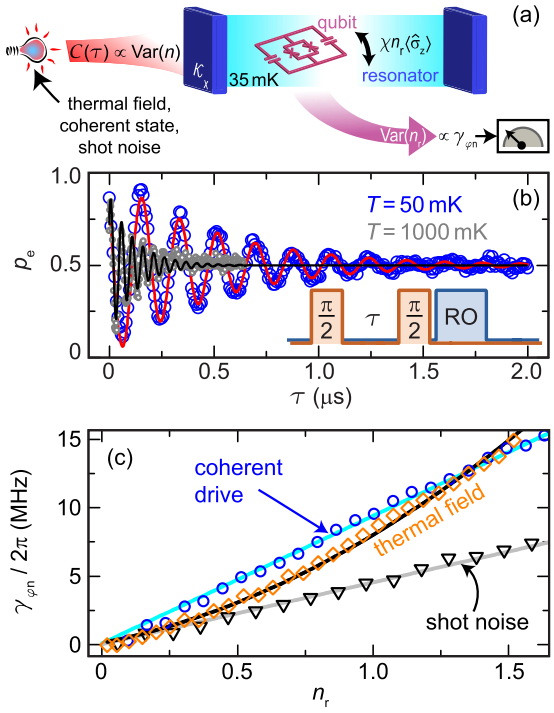

FIG. 2. (a) Sketch of the qubit setup. We measure the photon number variance $\mathrm{Var}(n)$ of microwave fields encoded in the photon correlator $\mathcal{C}(\tau)$ by detecting the dephasing rate $\gamma_{\varphi n}$ of a superconducting qubit. (b) Qubit excited state probability p_e for a Ramsey experiment plotted versus waiting time τ between two $\pi/2$ pulses. The solid lines are exponentially decaying sinusoidal fits. Inset: Ramsey pulse sequence followed by a readout (RO) pulse. (c) Qubit dephasing rates $\gamma_{\varphi n}$ of prototypical input fields plotted versus the average resonator population n_r, which is calibrated in an ac Stark shift measurement [51]. Solid lines are fits using Eqs. (1)–(3).

signals with white spectrum, $\tilde{\kappa} = \kappa_x$ corresponds to the energy decay rate of the resonator. Nevertheless, the thermal correlator $\mathcal{C}^{\mathrm{th}}(\tau) = (n_r^2 + n_r)\exp(-\kappa_x\tau)$ can be distinguished from the shot noise correlator $\mathcal{C}^{\mathrm{sh}}(\tau) = n_r\exp(-\kappa_x\tau)$ via their photon number variance. Remarkably, despite sharing a Poissonian photon statistics, $\mathcal{C}^{\mathrm{sh}}(\tau)$ differs from the coherent state correlator, $\mathcal{C}^{\mathrm{coh}}(\tau) = n_r\exp(-\kappa_x\tau/2)$, because the latter decays at the amplitude decay rate, $\tilde{\kappa} = \kappa_x/2$. All three correlators generate a shift $\delta\varphi(\tau)$ of the qubit phase, whose second moment [66], $\langle\delta\varphi^2\rangle = 4\chi^2\int_0^\tau \mathrm{d}\tau'\mathcal{C}(\tau')$, enters into the Ramsey decay envelope, $\exp[-\gamma_1(n_r)\tau/2 - \gamma_{\varphi 0}\tau - \langle\delta\varphi^2\rangle/2]$. Here, $\gamma_1(n_r)$ is the total qubit relaxation rate, and $\gamma_{\varphi 0}$ is the qubit dephasing rate due to all other noise sources except for those described by $\mathcal{C}(\tau)$. Assuming $\langle\delta\varphi^2\rangle/2 = \gamma_{\varphi n}(n_r)\tau$ and $|\chi| \ll \kappa_x$, the photon-field-induced dephasing rates approximate to [25,41,49,66–68]

$$\gamma^{\mathrm{th}}_{\varphi n}(n_r) = \kappa_x\theta_0^2(n_r^2 + n_r) \equiv s_0^{\mathrm{th}}(n_r^2 + n_r), \qquad (1)$$

$$\gamma_{\varphi n}^{\mathrm{coh}}(n_r) = 2\kappa_x\theta_0^2 n_r \equiv s_0^{\mathrm{coh}} n_r, \tag{2}$$

$$\gamma_{\varphi n}^{\mathrm{sh}}(n_r) = \kappa_x\theta_0^2 n_r \equiv s_0^{\mathrm{sh}} n_r. \tag{3}$$

Here, $\theta_0 \equiv \tan^{-1}(2\chi/\kappa_x)$ is the accumulated phase of the resonator photons due to the interaction with the qubit. The factor two between $\gamma_{\varphi n}^{\mathrm{coh}}$ and $\gamma_{\varphi n}^{\mathrm{sh}}$ reflects the fact that the impact of the fluctuations onto the qubit is larger if the correlator decays slower. As a consequence of Eqs. (1)–(3), measurements of the Ramsey decay rate, $\gamma_2(n_r) = \gamma_1(n_r)/2 + \gamma_{\varphi 0} + \gamma_{\varphi n}(n_r)$, allow us to extract $\mathrm{Var}(n_r)$ after correcting $\gamma_2(n_r)$ for $\gamma_1(n_r)$, obtained from an independent measurement [28,51]. We emphasize that during our sweeps of the attenuator temperature, the sample box is stabilized at 35 mK. Therefore, $\gamma_{\varphi 0}$ can be taken as a constant and we can extract $\gamma_{\varphi n}$ from the decay envelope of a Ramsey time trace.

In the absence of external microwave fields, the transmon qubit is relaxation limited with the rates $\gamma_1(n_r \simeq 0)/2\pi \simeq 4$ MHz and $\gamma_2(n_r \simeq 0)/2\pi \simeq 2$ MHz. In Figure 2(b), we show the Ramsey time traces for the attenuator temperatures $T = 50$ mK and $T = 1$ K. As expected, the latter shows a significantly increased Ramsey decay rate. A systematic temperature sweep reveals $\gamma_{\varphi n}^{\mathrm{th}}(n_r) \propto n_r^2 + n_r$, as displayed in Fig. 2(c). For small photon numbers, $n_r \lesssim 0.5$, the dephasing rate approaches a linear trend with slope $s_0^{\mathrm{th}} \equiv \partial\gamma_{\varphi n}^{\mathrm{th}}/\partial n_r|_{n_r=0}$. This finite slope clearly allows us to rule out the validity of the classical limit $\mathrm{Var}(n_r) = n_r^2$ in this regime. From a fit of Eq. (1) to the data, we find $s_0^{\mathrm{th}}/2\pi = 3.9$ MHz, which is marginally enhanced compared to the expected value $\kappa_x\theta_0^2/2\pi = 3.4$ MHz. Because the enhancement of s_0^{th} cannot be linked to the finite cavity pull $|\chi/\kappa_x| \simeq 0.3$, we attribute it to thermal photons n_n^{th} emitted from attenuators at higher temperature stages [51]. Applying a beam splitter model to calculate $\mathrm{Var}(n_r + n_n^{\mathrm{th}})$ yields the reasonable contribution of $n_n^{\mathrm{th}} = 0.15$, corresponding to an effective mode temperature of approximately 140 mK.

As a cross-check for our setup, we confirm the well-explored [23,26,41,66] linear variance of fields with Poissonian photon statistics. To this end, we first expose the resonator to shot noise emitted at room temperature by the AFG. As shown in Fig. 2(c), we indeed find a constant slope $s^{\mathrm{sh}} \equiv \partial\gamma_{\varphi n}^{\mathrm{sh}}/\partial n_r \simeq 2\pi \times 4.6$ MHz, which is in reasonable agreement with s_0^{th}. In terms of additional thermal population and effective mode temperature, we obtain $n_n^{\mathrm{sh}} \simeq 0.19 \approx n_n^{\mathrm{th}}$ and 150 mK, respectively. In the next step, we investigate measurement-induced dephasing caused by coherent states. We again find a linear slope $s^{\mathrm{coh}} \equiv \partial\gamma_{\varphi n}^{\mathrm{coh}}/\partial n_r \simeq 2\pi \times 9.3$ MHz. Although both coherent states and shot noise exhibit Poissonian statistics, we can reliably distinguish between the two of them using the fact that $s^{\mathrm{coh}} \simeq 2s^{\mathrm{sh}}$. This discrimination shows that the qubit dephasing rate directly reflects the temporal dependence of photon-photon correlators. The excellent quantitative agreement is also reflected in $n_n^{\mathrm{coh}} = n_n^{\mathrm{sh}}$, i.e., identical Fano factors [45], $\mathcal{F} \equiv \mathrm{Var}(n_r)/n_r \simeq 1.1$.

In order to complement our studies of thermal microwaves, we directly probe field correlations with the dual-path state reconstruction method [16–18,69]. This approach is motivated by the prediction that a beam splitter transfers the photon statistics of two uncorrelated inputs into correlations between its two outputs [70]. We use the setup depicted in Fig. 3(a), where a cryogenic beam splitter equally divides the signal along two paths, which are subsequently amplified independently. From their averaged auto- and cross-correlations, we retrieve all signal moments $\langle(\hat{a}^\dagger)^n\hat{a}^m\rangle$ up to fourth order ($0 \le n+m \le 4$, with n, $m \in \mathbb{N}_0$) in terms of the annihilation and creation operators, $\hat{a}$ and $\hat{a}^\dagger$. To calibrate the average photon number, $n_{\mathrm{bs}} = \langle\hat{a}^\dagger\hat{a}\rangle \propto n(T)$, at the input of the beam splitter, we

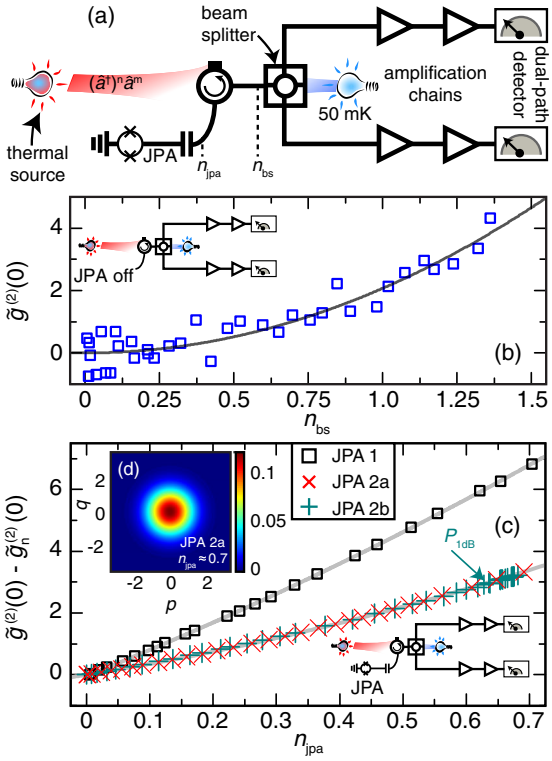

FIG. 3. (a) Sketch of the dual-path setup, which we use to probe field correlations between two amplification chains behind a cryogenic microwave beam splitter. We can switch the JPA on and off. (b) Unnormalized second-order correlation function $\tilde{g}^{(2)}(0)$ plotted versus photon number n_{bs} at the beam splitter input without using the JPA. The solid line is a fit to the data using the function $\tilde{g}^{(2)}(0) = \rho n_{\mathrm{bs}}^2$. (c) Unnormalized second-order correlation function $\tilde{g}^{(2)}(0)$ corrected for the constant offset $\tilde{g}_n^{(2)}(0)$ and plotted versus the photon number n_{jpa} at the JPA input. For the measurements of JPA 2a and JPA 2b, we use slightly different operating points, described in detail in Ref. [51]. (d) Wigner function reconstruction referred to the input of the JPA for a thermal state.

perform a Planck spectroscopy experiment [16] (see Ref. [51] for details). Notwithstanding the very different experimental requirements in the microwave regime, direct correlation measurements on propagating light fields are inspired from quantum optics. For this reason, we characterize the photon number variance of the thermal microwave fields via the unnormalized correlation function,

$$\tilde{g}^{(2)}(0) \equiv n_{\mathrm{bs}}^2 g^{(2)}(0) = \mathrm{Var}(n_{\mathrm{bs}}) - n_{\mathrm{bs}} + n_{\mathrm{bs}}^2. \quad (4)$$

As shown in Fig. 3(b), the correlation function $\tilde{g}^{(2)}(0)$ of the thermal source follows the expected quadratic behavior. A numerical fit of the polynomial function, $\tilde{g}^{(2)}(0) = \rho n_{\mathrm{bs}}^2$, using ρ as a free parameter, yields $\rho = 2.07$. This result coincides nicely with $\tilde{g}^{(2)}(0) = 2n_{\mathrm{bs}}^2$, predicted for thermal states by Eq. (4). In the same way as with the qubit setup, we are therefore able to reliably map out the $n^2 + n$ dependence and not only the classical n^2 limit experimentally found in earlier work [15].

To lower the statistical scatter of the data points in Fig. 3(b), we repeat the correlation measurement using a JPA operated in the phase-insensitive mode. In this mode, the JPA works as a near-quantum-limited, phase-preserving amplifier [21] with power gain $G \gg 1$. At the input of the beam splitter, one then obtains $n_{\mathrm{bs}} \approx G(n_{\mathrm{jpa}} + n_n + 1)$. Here, $n_{\mathrm{jpa}} \propto n(T)$ are the signal photons and n_n are the noise photons added by the JPA, which we again obtain from a Planck spectroscopy experiment [51]. We compare measurements using two different JPAs (JPA 1 and JPA 2), based on frequency-tunable quarter-wavelength resonators with operating frequencies $\omega_{\mathrm{jpa}}/2\pi \simeq 5.35$ GHz and typical gains $G \simeq 15$ dB. To characterize the noise referred to the input of the JPA, we analyze the modified correlation function

$$\tilde{g}^{(2)}(0) = 2(n_{\mathrm{jpa}} + n_n + 1)^2, \quad (5)$$

which can be derived from an input-output model for the JPA. In our model, we assume that the JPA noise is thermal, i.e., $\mathrm{Var}(n_n) = n_n^2 + n_n$. Then, there is a $n_{\mathrm{jpa}}-$ independent offset $\tilde{g}_n^{(2)}(0) = 2n_n^2 + 4n_n + 2$ in Eq. (5) due to the JPA gain and noise.

In Fig. 3(c), we plot the experimentally obtained correlations $\tilde{g}^{(2)}(0) - \tilde{g}_n^{(2)}(0)$ versus the photon number n_{jpa} at the JPA input. From fits to the formula $\rho n_{\mathrm{jpa}}^2 + \xi n_{\mathrm{jpa}}$, we find $\rho \simeq 2.2$ in all three data sets in agreement with the expected value of $\rho = 2$. Therefore, also the JPA assisted measurements confirm super-Poissonian statistics of the thermal fields. From the fits, we also find that the values of ξ are reduced by a factor of approximately 2 compared to the expected value $4 + 4n_n$. This observation is confirmed by the values extracted for $\tilde{g}_n^{(2)}(0)$, which deviate to a similar extent. Assuming that the photon statistics of the signal photons n_{jpa} is not changed by the JPA, the reduced experimental values suggest that the amplified noise contains a significant contribution $\mathrm{Var}(n_n) = n_n^2$. This classical contribution is power independent and unaffected when the JPAs exceed their 1 dB compression point $\mathcal{P}_{1\,\mathrm{dB}} \simeq -130$ dB m [see Fig. 3(c)]. We stress that the amplified fields are still Gaussian and show no squeezing effects between the two quadratures, $\hat{p} = \imath(\hat{a}^\dagger - \hat{a})/2$ and $\hat{q} = (\hat{a}^\dagger + \hat{a})/2$ [see Fig. 3(d)]. As shown in Ref. [51], we find $\mathrm{Var}(\hat{p}) = \mathrm{Var}(\hat{q})$ for the complete temperature range.

Finally, we compare the performance of the qubit and the dual-path setup. Although we operate on and below the single-photon level, the qubit and the dual-path setup (without JPA) systematically reproduce the $n^2 + n$ law with a high accuracy. Currently, the statistical spread for the qubit setup is one order of magnitude lower than the one for the dual-path setup. The accuracy of the qubit setup is limited by the Fano factor $\mathcal{F} \simeq 1.1$ of the setup and by the low-frequency variations of the qubit relaxation rate described in Ref. [28]. Their standard deviation of 5% well explains the spread of the experimental data points in Fig. 2(c). Assuming that these variations decrease proportionally to the qubit decoherence rate, we estimate that for the best performing superconducting qubits [49], the accuracy can be improved by at least two orders of magnitude. The dual-path setup (without the JPA) is limited by the data processing rate of our digitizer card and by the noise temperature $T_n \simeq 3$ K of the cryogenic amplifiers. When the JPA is on, the noise temperature of these amplifiers is insignificant. While our measurements including a JPA decrease the statistical spread by two orders of magnitude, they also introduce a systematic error due to uncertainties in the JPA noise statistics. Concerning adaptability, the dual-path setup, in principle, gives access to all signal moments, whereas the qubit is limited to amplitude and power correlations.

In conclusion, we have quantitatively characterized the photon number variance of propagating thermal microwaves using two fundamentally different approaches: indirect measurements with a superconducting qubit-resonator system and direct ones with a dual-path detector. With both setups, we are able to quantitatively recover the $n^2 + n$ photon number variance of thermal fields in the single-photon regime with a high resolution in comparison with existing experimental achievements [15]. In particular, we analyze the resolution limits and find that they may improve by several orders of magnitude in both setups. For our current dual-path setup, we make the remarkable observation that noise added by the JPAs has a significant contribution with $\mathrm{Var}(n) = n^2$. Our results demonstrate that the three types of propagating microwave states that we investigate are reliably distinguishable below the single-photon level in an experiment by their photon statistics. Therefore, both setups are promising candidates to explore decoherence mechanisms, possibly limiting

high-performance superconducting qubits [49,50] and the properties of more advanced quantum microwave states.

The JPAs used in this work are kindly provided by K. Inomata (RIKEN Center for Emergent Matter Science), T. Yamamoto (NEC IoT Device Research Laboratories), and Y. Nakamura (RIKEN, RCAST at the University of Tokyo). We thank E. Solano, R. Di Candia, M. Sanz (Department of Physical Chemistry, University of the Basque Country) for fruitful discussions on the correlation measurement setup. We acknowledge financial support from the German Research Foundation through SFB 631 and FE 1564/1-1, EU projects CCQED, PROMISCE, the doctorate program ExQM of the Elite Network of Bavaria, and the International Max Planck Research School "Quantum Science and Technology."

*jan.goetz@wmi.badw.de
†rudolf.gross@wmi.badw.de

[1] D. Bouwmeester, J.-W. Pan, K. Mattle, M. Eibl, H. Weinfurter, and A. Zeilinger, Nature (London) **390**, 575 (1997).
[2] A. Furusawa, J. L. Sørensen, S. L. Braunstein, C. A. Fuchs, H. J. Kimble, and E. S. Polzik, Science **282**, 706 (1998).
[3] P. Kok, W. J. Munro, K. Nemoto, T. C. Ralph, J. P. Dowling, and G. J. Milburn, Rev. Mod. Phys. **79**, 135 (2007).
[4] S. L. Braunstein and P. van Loock, Rev. Mod. Phys. **77**, 513 (2005).
[5] U. L. Andersen, J. S. Neergaard-Nielsen, P. van Loock, and A. Furusawa, Nat. Phys. **11**, 713 (2015).
[6] R. Di Candia, K. G. Fedorov, L. Zhong, S. Felicetti, E. P. Menzel, M. Sanz, F. Deppe, A. Marx, R. Gross, and E. Solano, Eur. Phys. J. Quant. Tech. **2**, 25 (2015).
[7] S. Lloyd, Science **321**, 1463 (2008).
[8] S.-H. Tan, B. I. Erkmen, V. Giovannetti, S. Guha, S. Lloyd, L. Maccone, S. Pirandola, and J. H. Shapiro, Phys. Rev. Lett. **101**, 253601 (2008).
[9] E. D. Lopaeva, I. Ruo Berchera, I. P. Degiovanni, S. Olivares, G. Brida, and M. Genovese, Phys. Rev. Lett. **110**, 153603 (2013).
[10] S. Barzanjeh, S. Guha, C. Weedbrook, D. Vitali, J. H. Shapiro, and S. Pirandola, Phys. Rev. Lett. **114**, 080503 (2015).
[11] N. Y. Yao, L. Jiang, A. V. Gorshkov, Z.-X. Gong, A. Zhai, L.-M. Duan, and M. D. Lukin, Phys. Rev. Lett. **106**, 040505 (2011).
[12] N. Y. Yao, Z.-X. Gong, C. R. Laumann, S. D. Bennett, L.-M. Duan, M. D. Lukin, L. Jiang, and A. V. Gorshkov, Phys. Rev. A **87**, 022306 (2013).
[13] J. B. Brask, G. Haack, N. Brunner, and M. Huber, New J. Phys. **17**, 113029 (2015).
[14] Z.-L. Xiang, M. Zhang, L. Jiang, and P. Rabl, arXiv:1611.10241.
[15] J. Gabelli, L.-H. Reydellet, G. Fève, J.-M. Berroir, B. Placais, P. Roche, and D. C. Glattli, Phys. Rev. Lett. **93**, 056801 (2004).
[16] M. Mariantoni, E. P. Menzel, F. Deppe, M. A. Araque Caballero, A. Baust, T. Niemczyk, E. Hoffmann, E. Solano, A. Marx, and R. Gross, Phys. Rev. Lett. **105**, 133601 (2010).
[17] E. P. Menzel, F. Deppe, M. Mariantoni, M. A. Araque Caballero, A. Baust, T. Niemczyk, E. Hoffmann, A. Marx, E. Solano, and R. Gross, Phys. Rev. Lett. **105**, 100401 (2010).
[18] E. P. Menzel, R. Di Candia, F. Deppe, P. Eder, L. Zhong, M. Ihmig, M. Haeberlein, A. Baust, E. Hoffmann, D. Ballester, K. Inomata, T. Yamamoto, Y. Nakamura, E. Solano, A. Marx, and R. Gross, Phys. Rev. Lett. **109**, 250502 (2012).
[19] K. G. Fedorov, L. Zhong, S. Pogorzalek, P. Eder, M. Fischer, J. Goetz, E. Xie, F. Wulschner, K. Inomata, T. Yamamoto, Y. Nakamura, R. Di Candia, U. Las Heras, M. Sanz, E. Solano, E. P. Menzel, F. Deppe, A. Marx, and R. Gross, Phys. Rev. Lett. **117**, 020502 (2016).
[20] F. Mallet, M. A. Castellanos-Beltran, H. S. Ku, S. Glancy, E. Knill, K. D. Irwin, G. C. Hilton, L. R. Vale, and K. W. Lehnert, Phys. Rev. Lett. **106**, 220502 (2011).
[21] L. Zhong, E. P. Menzel, R. Di Candia, P. Eder, M. Ihmig, A. Baust, M. Haeberlein, E. Hoffmann, K. Inomata, T. Yamamoto, Y. Nakamura, E. Solano, F. Deppe, A. Marx, and R. Gross, New J. Phys. **15**, 125013 (2013).
[22] C. Macklin, K. O'Brien, D. Hover, M. E. Schwartz, V. Bolkhovsky, X. Zhang, W. D. Oliver, and I. Siddiqi, Science **350**, 307 (2015).
[23] S. Virally, J. O. Simoneau, C. Lupien, and B. Reulet, Phys. Rev. A **93**, 043813 (2016).
[24] C. Eichler, D. Bozyigit, C. Lang, L. Steffen, J. Fink, and A. Wallraff, Phys. Rev. Lett. **106**, 220503 (2011).
[25] A. A. Clerk and D. W. Utami, Phys. Rev. A **75**, 042302 (2007).
[26] A. P. Sears, A. Petrenko, G. Catelani, L. Sun, H. Paik, G. Kirchmair, L. Frunzio, L. I. Glazman, S. M. Girvin, and R. J. Schoelkopf, Phys. Rev. B **86**, 180504 (2012).
[27] K. W. Murch, S. J. Weber, K. M. Beck, E. Ginossar, and I. Siddiqi, Nature (London) **499**, 62 (2013).
[28] J. Goetz, F. Deppe, P. Eder, M. Fischer, M. Müting, J. Puertas Martínez, S. Pogorzalek, F. Wulschner, E. Xie, K. G. Fedorov, A. Marx, and R. Gross, arXiv:1609.07351.
[29] D. M. Meekhof, C. Monroe, B. E. King, W. M. Itano, and D. J. Wineland, Phys. Rev. Lett. **76**, 1796 (1996).
[30] M. Brune, F. Schmidt-Kaler, A. Maali, J. Dreyer, E. Hagley, J. M. Raimond, and S. Haroche, Phys. Rev. Lett. **76**, 1800 (1996).
[31] M. Hofheinz, E. M. Weig, M. Ansmann, R. C. Bialczak, E. Lucero, M. Neeley, A. D. O'Connell, H. Wang, J. M. Martinis, and A. N. Cleland, Nature (London) **454**, 310 (2008).
[32] D. I. Schuster, A. A. Houck, J. A. Schreier, A. Wallraff, J. M. Gambetta, A. Blais, L. Frunzio, J. Majer, B. Johnson, M. H. Devoret, S. M. Girvin, and R. J. Schoelkopf, Nature (London) **445**, 515 (2007).
[33] B. L. Morgan and L. Mandel, Phys. Rev. Lett. **16**, 1012 (1966).
[34] F. Arecchi, E. Gatti, and A. Sona, Phys. Lett. **20**, 27 (1966).
[35] P. K. Tan, G. H. Yeo, H. S. Poh, A. H. Chan, and C. Kurtsiefer, Astrophys. J. Lett. **789**, L10 (2014).
[36] R. Short and L. Mandel, Phys. Rev. Lett. **51**, 384 (1983).
[37] G. Rempe, F. Schmidt-Kaler, and H. Walther, Phys. Rev. Lett. **64**, 2783 (1990).

[38] F. Treussart, R. Alléaume, V. Le Floc'h, L. T. Xiao, J.-M. Courty, and J.-F. Roch, Phys. Rev. Lett. **89**, 093601 (2002).
[39] R. Hanbury Brown and R. Q. Twiss, Nature (London) **177**, 27 (1956).
[40] R. Hanbury Brown and R. Q. Twiss, Nature (London) **178**, 1046 (1956).
[41] D. I. Schuster, A. Wallraff, A. Blais, L. Frunzio, R.-S. Huang, J. Majer, S. M. Girvin, and R. J. Schoelkopf, Phys. Rev. Lett. **94**, 123602 (2005).
[42] A. A. Houck, D. I. Schuster, J. M. Gambetta, J. A. Schreier, B. R. Johnson, J. M. Chow, L. Frunzio, J. Majer, M. H. Devoret, S. M. Girvin, and R. J. Schoelkopf, Nature (London) **449**, 328 (2007).
[43] J. M. Fink, L. Steffen, P. Studer, L. S. Bishop, M. Baur, R. Bianchetti, D. Bozyigit, C. Lang, S. Filipp, P. J. Leek, and A. Wallraff, Phys. Rev. Lett. **105**, 163601 (2010).
[44] J.-C. Forgues, C. Lupien, and B. Reulet, Phys. Rev. Lett. **113**, 043602 (2014).
[45] C. Beenakker and M. Patra, Mod. Phys. Lett. A **13**, 337 (1999).
[46] Y. Blanter and M. Büttiker, Phys. Rep. **336**, 1 (2000).
[47] J. Koch, T. M. Yu, J. Gambetta, A. A. Houck, D. I. Schuster, J. Majer, A. Blais, M. H. Devoret, S. M. Girvin, and R. J. Schoelkopf, Phys. Rev. A **76**, 042319 (2007).
[48] T. Yamamoto, K. Inomata, M. Watanabe, K. Matsuba, T. Miyazaki, W. D. Oliver, Y. Nakamura, and J. S. Tsai, Appl. Phys. Lett. **93**, 042510 (2008).
[49] C. Rigetti, J. M. Gambetta, S. Poletto, B. L. T. Plourde, J. M. Chow, A. D. Córcoles, J. A. Smolin, S. T. Merkel, J. R. Rozen, G. A. Keefe, M. B. Rothwell, M. B. Ketchen, and M. Steffen, Phys. Rev. B **86**, 100506 (2012).
[50] F. Yan, S. Gustavsson, A. Kamal, J. Birenbaum, A. P. Sears, D. Hover, T. J. Gudmundsen, D. Rosenberg, G. Samach, S. Weber, J. L. Yoder, T. P. Orlando, J. Clarke, A. J. Kerman, and W. D. Oliver, Nat. Commun. **7**, 12964 (2016).
[51] See Supplemental Material at http://link.aps.org/supplemental/10.1103/PhysRevLett.118.103602 for details on the experimental setup and theoretical derivations, which includes Refs. [52–62].
[52] Y. Kano and E. Wolf, Proc. Phys. Soc. London **80**, 1273 (1962).
[53] C. L. Mehta, Il Nuovo Cimento **28**, 401 (1963).
[54] G. Lindblad, Commun. Math. Phys. **48**, 119 (1976).
[55] C. M. Caves, Phys. Rev. D **26**, 1817 (1982).
[56] J. Gambetta, A. Blais, M. Boissonneault, A. A. Houck, D. I. Schuster, and S. M. Girvin, Phys. Rev. A **77**, 012112 (2008).
[57] L. J. Klein, H. F. Hamann, Y.-Y. Au, and S. Ingvarsson, Appl. Phys. Lett. **92**, 213102 (2008).
[58] M. Boissonneault, J. M. Gambetta, and A. Blais, Phys. Rev. A **79**, 013819 (2009).
[59] A. A. Clerk, M. H. Devoret, S. M. Girvin, F. Marquardt, and R. J. Schoelkopf, Rev. Mod. Phys. **82** (2010).
[60] *Quantum Machines: Measurement and Control of Engineered Quantum Systems: Lecture Notes of the Les Houches Summer School*, edited by M. Devoret, B. Huard, R. Schoelkopf, and L. Cugliandolo (Oxford University Press, Oxford, 2014), Vol. 96, p. 231.
[61] B. A. Kochetov and A. Fedorov, Phys. Rev. B **92**, 224304 (2015).
[62] J. Goetz, F. Deppe, M. Haeberlein, F. Wulschner, C. W. Zollitsch, S. Meier, M. Fischer, P. Eder, E. Xie, K. G. Fedorov, E. P. Menzel, A. Marx, and R. Gross, J. Appl. Phys. **119**, 015304 (2016).
[63] C. W. Gardiner and A. S. Parkins, Phys. Rev. A **50**, 1792 (1994).
[64] A. Ridolfo, M. Leib, S. Savasta, and M. J. Hartmann, Phys. Rev. Lett. **109**, 193602 (2012).
[65] A. Blais, R.-S. Huang, A. Wallraff, S. M. Girvin, and R. J. Schoelkopf, Phys. Rev. A **69**, 062320 (2004).
[66] J. Gambetta, A. Blais, D. I. Schuster, A. Wallraff, L. Frunzio, J. Majer, M. H. Devoret, S. M. Girvin, and R. J. Schoelkopf, Phys. Rev. A **74**, 042318 (2006).
[67] P. Bertet, I. Chiorescu, C. Harmans, and J. Mooij, arXiv:cond-mat/0507290.
[68] P. Bertet, I. Chiorescu, G. Burkard, K. Semba, C. J. P. M. Harmans, D. P. DiVincenzo, and J. E. Mooij, Phys. Rev. Lett. **95**, 257002 (2005).
[69] R. Di Candia, E. P. Menzel, L. Zhong, F. Deppe, A. Marx, R. Gross, and E. Solano, New J. Phys. **16**, 015001 (2014).
[70] R. A. Campos, B. E. A. Saleh, and M. C. Teich, Phys. Rev. A **40**, 1371 (1989).